Article

Cell Reports

Müller Glial Cells Participate in Retinal Waves via Glutamate Transporters and AMPA Receptors

Graphical Abstract

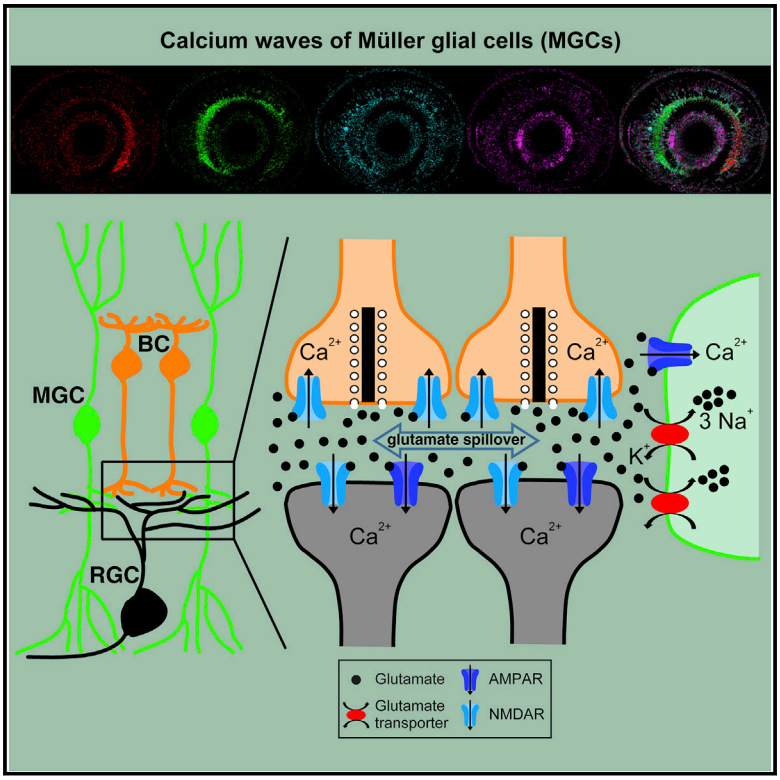

Authors

Rong-wei Zhang, Wen-jie Du, David A. Prober, Jiu-lin Du

Correspondence

rongweizhang@gmail.com (R.-w.Z.), forestdu@ion.ac.cn (J.-l.D.)

In Brief

The behavior and function of glial cells in spontaneous retinal waves remain unclear. Using *in vivo* calcium imaging and electrophysiological recording in larval zebrafish, Zhang et al. show that Müller glial cells can participate in and modulate retinal waves, respectively, via AMPA receptors and glutamate transporters on their own processes.

Highlights

- Müller glial cells (MGCs) display spontaneous wave activities
- AMPA receptors of MGCs mediate calcium activities in MGCs during retinal waves
- Glutamate transporters of MGCs modulate the occurrence of retinal waves
- MGCs can sense and regulate retinal waves

Zhang et al., 2019, Cell Reports *27*, 2871–2880
June 4, 2019
https://doi.org/10.1016/j.celrep.2019.05.011

CellPress

Cell Reports
Article

Müller Glial Cells Participate in Retinal Waves via Glutamate Transporters and AMPA Receptors

Rong-wei Zhang,[1,5,*] Wen-jie Du,[1] David A. Prober,[4] and Jiu-lin Du[1,2,3,*]
[1]Institute of Neuroscience, State Key Laboratory of Neuroscience, Center for Excellence in Brain Science and Intelligence Technology, Chinese Academy of Sciences, 320 Yue-Yang Road, Shanghai 200031, China
[2]School of Life Science and Technology, ShanghaiTech University, 319 Yue-Yang Road, Shanghai 200031, China
[3]School of Future Technology, University of Chinese Academy of Sciences, 19A Yu-Quan Road, Beijing 100049, China
[4]Division of Biology and Biological Engineering, California Institute of Technology, Pasadena, CA 91125, USA
[5]Lead Contact
*Correspondence: rongweizhang@gmail.com (R.-w.Z.), forestdu@ion.ac.cn (J.-l.D.)
https://doi.org/10.1016/j.celrep.2019.05.011

SUMMARY

Retinal waves, the spontaneous patterned neural activities propagating among developing retinal ganglion cells (RGCs), instruct the activity-dependent refinement of visuotopic maps. Although it is known that the wave is initiated successively by amacrine cells and bipolar cells, the behavior and function of glia in retinal waves remain unclear. Using multiple *in vivo* methods in larval zebrafish, we found that Müller glial cells (MGCs) display wave-like spontaneous activities, which start at MGC processes within the inner plexiform layer, vertically spread to their somata and endfeet, and horizontally propagate into neighboring MGCs. MGC waves depend on glutamatergic signaling derived from bipolar cells. Moreover, MGCs express both glia-specific glutamate transporters and the AMPA subtype of glutamate receptors. The AMPA receptors mediate MGC calcium activities during retinal waves, whereas the glutamate transporters modulate the occurrence of retinal waves. Thus, MGCs can sense and regulate retinal waves via AMPA receptors and glutamate transporters, respectively.

INTRODUCTION

Patterned spontaneous neural activities sweep across neighboring retinal ganglion cells (RGCs) in a wave-like manner during early development, called retinal waves (Meister et al., 1991; Wong, 1999). Retinal waves have been found in many vertebrate species, including fish, reptiles, birds, rodents, and primates (Ackman and Crair, 2014; Wong, 1999; Zhang et al., 2010). These wave-like neural activities can propagate via the optic nerve into the lateral geniculate nucleus and superior colliculus of rodents or the optic tectum of zebrafish (Ackman et al., 2012; Zhang et al., 2016) and are believed to play an instructive role in the activity-dependent refinement of visual topographic maps (Katz and Shatz, 1996; Kirkby et al., 2013). Besides RGCs, retinal bipolar cells (BCs) and amacrine cells (ACs) exhibit spontaneous wave-like activities and contribute to the initiation of retinal waves observed in RGCs at different developmental stages (Akrouh and Kerschensteiner, 2013; Ford et al., 2012; Zhang et al., 2016). Computational model and experimental evidence indicates that these wave-like correlated activities between BCs and RGCs or between ACs and RGCs may underlie the formation of early retinal circuitries via a Hebbian mechanism (Butts et al., 2007; Wei et al., 2012).

Müller glial cells (MGCs), the principal glial cells in the vertebrate retina, span across the entire thickness of the retina. They form close contacts with retinal neurons, penetrate into neighboring synaptic clefts, and contribute to the maintenance of tissue structure (Newman and Reichenbach, 1996; Ramon y Cajal, 1972; Williams et al., 2010). Intensive studies on adult animals have revealed multiple functions of MGCs in retinal physiology, including clearance of metabolic waste, regulation of blood vessel dilation or constriction, modulation of neuronal activities, and even passing of light (Franze et al., 2007; Halassa and Haydon, 2010; Newman, 2015; Reichenbach and Bringmann, 2013). A recent study in mice reported that the stalk and lateral processes in the inner plexiform layer (IPL) of RGCs show calcium transients correlated with the activities of RGCs in early development that are mediated by acetylcholine or glutamate receptors (Rosa et al., 2015).

To further examine the existence and role of wave-like activities in MGCs, we used the zebrafish larva as an animal model, because the optical transparency and external fertilization of the fish embryo make it feasible for *in vivo* investigation of the activities of a population of MGCs in the intact retina. Our previous studies showed that retinal waves in zebrafish exist within a narrow developmental window from 2.5 to 3.5 days post-fertilization (dpf) (Zhang et al., 2010, 2016). In contrast to three distinct stages of retinal waves in mammals that depend on different synaptic signals (Blankenship and Feller, 2010; Wong, 1999), retinal waves in zebrafish are mainly initiated by glutamate released from the axon terminals of BCs, propagate via gap junctions between BCs, and are slightly affected by cholinergic signaling (Zhang et al., 2016). In the present work, we applied multiple *in vivo* techniques, including whole-cell recording and calcium imaging, and found that MGCs exhibited spontaneous rhythmic wave-like activities. These MGC waves were dependent on glutamatergic signaling. Moreover, we found that MGCs express

glia-specific glutamate transporters and the α-amino-3-hydroxy-5-methyl-4-isoxazolepropionic acid (AMPA) subtype of glutamate receptors. Blockade of AMPA receptors abolished MGC calcium activities during retinal waves, whereas manipulation of glial glutamate transporters affected the occurrence of retinal waves. These results suggest that MGCs detect the existence of retinal waves through AMPA receptors and modulate the occurrence of retinal waves through glutamate transporters.

RESULTS

Müller Glial Cells of Zebrafish Larvae Exhibit Wave-like Spontaneous Activities

To examine whether MGCs have wave-like spontaneous activities during early development, we performed *in vivo* whole-cell recordings of MGCs in the transgenic zebrafish Tg(GFAP:eGFP) at 3 dpf, in which the eGFP is specifically expressed in glial cells, including MGCs, via the promoter of the zebrafish *glial fibrillary acid protein* (*gfap*) gene (Bernardos et al., 2007; Williams et al., 2010) (Figures 1A and S1A). MGCs exhibited spontaneous periodic giant depolarizing potentials (GDPs) under current-clamp mode or giant inward currents (GICs) under voltage-clamp mode (Figure 1B), similar to the wave-like electrical activities observed in zebrafish BCs and RGCs (Zhang et al., 2010, 2016). The amplitude of MGC GDPs ranged from 3.0 to 39.8 mV, with an average of 16.3 ± 0.7 mV (Figure S1B; n = 149 events from 28 MGCs, means ± SEMs). The mean event duration and inter-event interval of MGC GDPs were 7.9 ± 0.2 and 145.7 ± 8.0 s, respectively (Figures S1C and S1D), comparable with those of BC and RGC waves (Zhang et al., 2016). By using double whole-cell recordings of an MGC and an RGC, we found that the MGC and RGC displayed correlated spontaneous giant electrical activities in 11 of 18 double recordings (Figures 1C and 1D). Furthermore, we performed double whole-cell recordings of two neighboring MGCs and found that these cells showed correlated spontaneous activities in 5 of 10 double recordings (Figures 1E and 1F). Moreover, these giant electrical activities of MGCs occurred only during 3.0–3.5 dpf (Figure 1G), the same time window as the BC and RGC waves (Zhang et al., 2016).

To demonstrate that these wave-like activities can propagate across populations of MGCs, we then performed *in vivo* time-lapse two-photon calcium imaging on 3-dpf Tg(GFAP:GCaMP2) larvae, in which the genetically encoded calcium indicator GCaMP2 is specifically expressed in glial cells. Populations of MGCs showed spontaneous rhythmic calcium waves, which started at their processes within the IPL, then vertically spread into their endfeet and even somata, and horizontally propagated into neighboring MGCs (Figures 2A and 2B; Video S1). Consistent with the initiation at the temporal retina of BC and RGC waves (Zhang et al., 2016), we found that MGC calcium waves also preferentially started at the IPL of the temporal retina (45 waves from 6 retinae; Figures 2C and 2D). Consistent with the time window of the giant electrical activities of MGCs (see Figure 1G), the calcium waves of MGCs also occurred during 3.0–3.5 dpf (Figure 2E).

MGC Waves Depend on BC Activation

Our previous work indicated that retinal waves observed in the BCs and RGCs of zebrafish are initiated by glutamate released from the axon terminals of BCs (Zhang et al., 2016). Based the consistency of the spatiotemporal pattern of retinal waves observed in MGCs (see Figures 1 and 2), BCs and RGCs (see Figures 1 and 7 in Zhang et al., 2016), we hypothesized that, similar to BC and RGC waves, MGC waves may also be dependent on BC activation and relevant glutamatergic signals. We first blocked ionotropic glutamatergic transmission by bath application of 6-cyano-7-nitroquinoxaline-2,3-dione (CNQX, 50 μM), an antagonist of AMPA receptors, and DL-2-amino-5-phosphonovaleric acid (APV, 50 μM), an antagonist of the *N*-methyl-D-aspartate (NMDA) subtype of glutamate receptors. Consistent with the blockade of BC waves by APV and CNQX (Zhang et al., 2016), both calcium waves and electrical GDPs of MGCs were totally abolished by glutamatergic transmission blockade (Figures 3A–3D and 3G; $p < 0.01$). In addition, the blockade of nicotinic or muscarinic acetylcholine receptors by hexamethonium (HEX; 100 μM) or atropine (2 μM), respectively, did not significantly affect the occurrence of MGC waves (Figures 3E–3G), although the amplitude of MGC waves was slightly reduced by HEX application (Figure 3H). Therefore, MGC waves are largely dependent on glutamatergic but not cholinergic receptors.

As BCs are the major source of glutamatergic signals in the inner retina of vertebrates (Euler et al., 2014), it is reasonable that the MGC wave may originate from BCs. We thus applied L-2-amino-4-phosphonobutyric acid (L-AP4, 50 μM), an agonist of metabotropic glutamate receptors (mGluRs) group III, to manipulate the activities of BCs. L-AP4 can hyperpolarize ON-type BCs due to the activation of mGluR6, which mainly distributes on BC dendrites in the retina (Snellman et al., 2008). We found that L-AP4 application largely suppressed the occurrence of both BC and RGC waves (Figures S2A, S2B, and S2D; $p < 0.001$), indicating the necessity of ON-type BCs in the generation of retinal waves. The occurrence of MGC waves was consistently significantly suppressed by L-AP4 application (Figures S2C and S2D; $p < 0.01$). These results suggest that MGC waves are largely dependent on BC activation-associated glutamatergic signaling.

MGCs Express Glia-Specific Glutamate Transporters and AMPA Receptors

Previous studies show that glutamate released from BCs activates ionotropic glutamate receptors on the axon terminals of BCs and the dendrites of RGCs, and triggers glutamatergic retinal waves in BCs and RGCs (Blankenship et al., 2009; Firl et al., 2013; Zhang et al., 2016). Therefore, we speculated that glutamate may diffuse out of the synaptic cleft during retinal waves and activate MGCs. To test this hypothesis, we performed *in vivo* whole-cell recordings on the soma of MGCs and puffed glutamate onto their processes within the IPL. Under blockade of synaptic transmission by adding Co^{2+} (5 mM) in the external solution, glutamate puffing induced the depolarization of MGCs when the membrane potential of the cell was maintained at approximately −60 mV (Figure 4A). This depolarization could be largely suppressed by 1 μM (2S, 3S)-3-[3-[4-(trifluoromethyl) benzoylamino]benzyloxy]aspartate (TFB-TBOA) (15.2% ± 3.1% of control, $p < 0.01$), a selective inhibitor of subtypes 1 and 2 of the excitatory amino acid transporters EAAT1 and EAAT2 (also called glutamate and aspartate transporter [GLAST] and

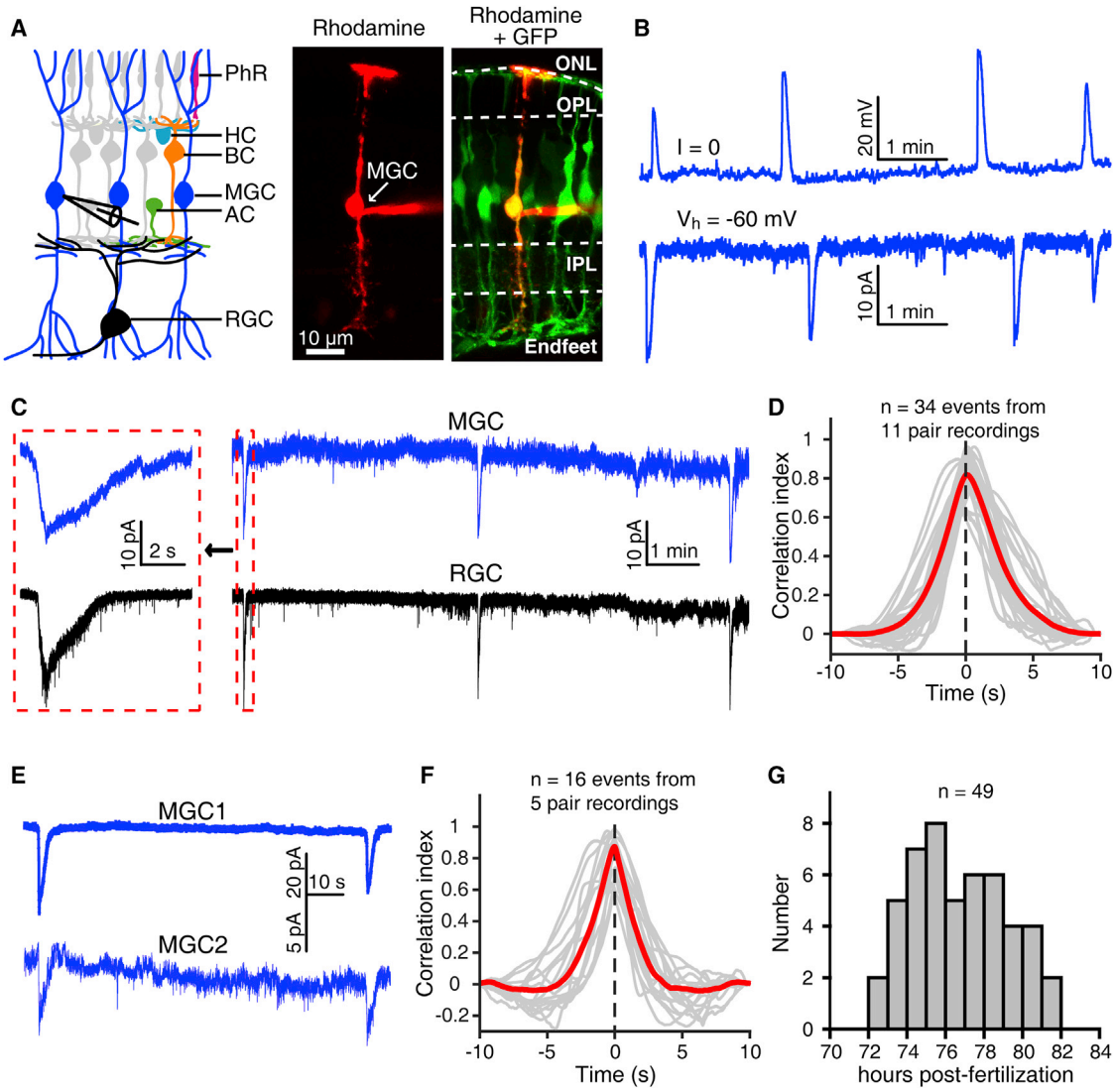

Figure 1. Müller Glial Cells of Zebrafish Larvae Exhibit Spontaneous Rhythmic Electrical Activities

(A) Left, schematic of vertebrate retinal cellular structure. Right, confocal images showing the morphology of a Müller glial cell (MGC) when 1% rhodamine (red) was loaded into the MGC via a whole-cell recording pipette in a 3-dpf Tg(GFAP:eGFP) larva. AC, amacrine cell; BC, bipolar cell; HC, horizontal cell; IPL, inner plexiform layer; MGC, Müller glial cell; ONL, outer nuclear layer; OPL, outer plexiform layer; PhR, photoreceptor; RGC, retinal ganglion cell.

(B) Spontaneous rhythmic giant activities of an MGC monitored with whole-cell recording in a 3-dpf larva under current- (top) or voltage-clamp mode (at −60 mV, bottom).

(C) Correlated spontaneous giant activities between an MGC and an RGC monitored with double whole-cell recordings. Left, enlarged view of the correlated events shown in the dashed boxes.

(D) Cross-correlation between MGCs' and RGCs' spontaneous giant activities. The 34 events obtained from 11 pairs of 1 MGC and 1 RGC were analyzed. The gray lines represent the cross-correlation of single events, and the red line indicates the average.

(E) Correlated spontaneous electrical activities between two nearby MGCs monitored with double whole-cell recordings. Both cells were held at −60 mV.

(F) Cross-correlation between MGCs' spontaneous giant activities. The 16 events obtained from 5 MGC pairs were analyzed. The gray lines represent the cross-correlation of single events, and the red line indicates the average.

(G) Temporal distribution of the occurrence of MGCs' spontaneous giant electrical activities. Whole-cell recording data were obtained from 49 larvae.

glutamate transporter [GLT]-1, respectively) (Tsukada et al., 2005). Previous studies showed that in larval zebrafish, EAAT2 but not EAAT1 was consistently found to be expressed in the retina (Gesemann et al., 2010; Niklaus et al., 2017) and that both EAAT2a and 2b subtypes are expressed in MGCs but not in RGCs (Niklaus et al., 2017).

Furthermore, we found the glutamate-induced response in MGCs was partially suppressed by CNQX (78.5% ± 5.0% of control, $p < 0.05$), but not significantly affected by APV (94.5% ± 2.1% of control, $p = 0.09$) (Figures 4A and 4B), suggesting that MGC responses to glutamate are mediated by both glutamate transporters and AMPA receptors. Puffing of glutamate or AMPA

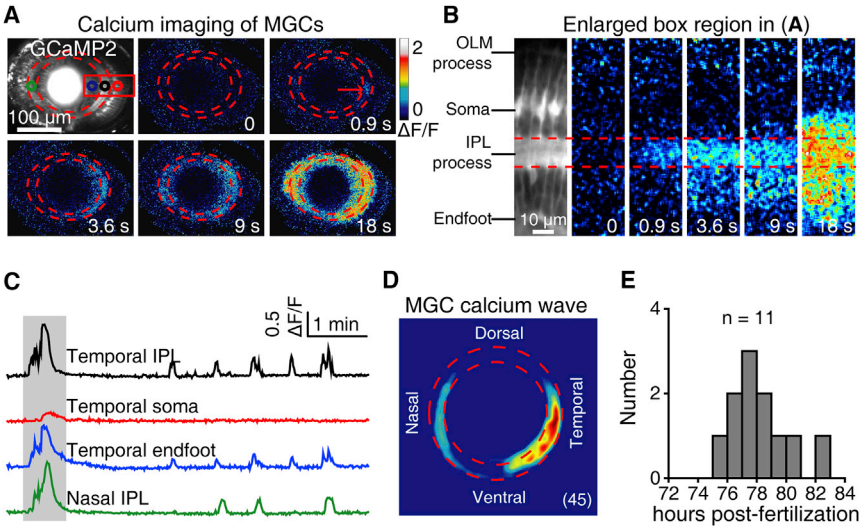

Figure 2. Müller Glial Cells of Zebrafish Larvae Display Spontaneous Calcium Waves

(A) Pseudocolor time-lapse two-photon images showing a spontaneous calcium wave of MGCs in a 3-dpf Tg(GFAP:GCaMP2) larva. The two red dashed circles indicate the boundaries of the IPL, and the red arrow indicates the initiation site of the wave.

(B) Enlarged region of the red box in (A), showing the vertical propagation from MGC processes in the IPL to their endfeet and somata. IPL, inner plexiform layer; OLM, outer limiting membrane.

(C) Calcium activities of four regions of interest in (A, colored circles). The shadowed area marks the period of images shown in (A).

(D) Superposition of the initiation site of 45 MGC calcium waves from 6 larvae.

(E) Temporal distribution of the occurrence of spontaneous MGC calcium waves. Calcium imaging data were obtained from 11 larvae.

consistently induced large responses in MGCs (11.9 ± 2.6 mV for glutamate and 6.0 ± 1.2 mV for AMPA), but puffing of NMDA evoked small responses (0.4 ± 0.3 mV) (Figures 4C and 4D). In contrast to the reversal potential of AMPA receptors at approximately 0 mV (Malinow and Malenka, 2002), we further found that glutamate application always evoked an inward current, even when the MGC was held above 0 mV (Figures 4E and 4F), a typical property of glutamate transporter-carried currents (Schwartz and Tachibana, 1990). These data indicate that MGCs in larval zebrafish express both functional glutamate transporters and AMPA receptors.

AMPA Receptors Mediate Calcium Activities of MGCs during Retinal Waves

As the activation of glial glutamate transporters causes the influx of three Na^+ and the efflux of one K^+ without the flow of Ca^{2+}, we speculated that the Ca^{2+} increase in MGCs during retinal waves may be due to the activation of AMPA receptors. We thus bath applied CNQX (50 μM) and found that AMPA receptor blockade totally suppressed spontaneous calcium waves in MGCs (Figures 5A and 5B; 3.8% ± 2.5% of control, $p < 0.01$). Under blockade of synaptic transmission by adding Co^{2+} in the external solution, glutamate-induced calcium activities in MGCs were largely suppressed by CNQX treatment (Figures 5C and 5D; 16.6% ± 3.9% of control, $p < 0.01$), but not by TFB-TBOA (Figure S3; 106.9% ± 4.2% of control, $p = 0.32$). Glutamate-induced calcium transients of MGCs in immature mice were also consistently suppressed by the antagonist of AMPA receptors, but not by that of NMDA receptors (Rosa et al., 2015). Furthermore, we found that bath application of 100 μM Naspm trihydrochloride, a selective calcium-permeable AMPA receptor antagonist (Budisantoso et al., 2012; Droste et al., 2017), largely suppressed the occurrence of spontaneous calcium waves in MGCs (Figures 5E and 5F; 24.5% ± 1.7% of control, $p < 0.01$) and reduced the glutamate-induced calcium activities of MGCs (Figures 5G and 5H; 47.0% ± 7.1% of control, $p < 0.01$). These results indicate that the Ca^{2+} activity of MGCs during retinal waves may be mainly mediated by the calcium-permeable AMPA receptors of MGCs (Peng et al., 1995; Yazulla and Studholme, 2001).

Although AMPA receptors are important for MGC calcium activities, we found that they play only a minor role in the electrical activities of MGCs during retinal waves (Figure S4). Bath application of CNQX significantly reduced both the frequency (53.2% ± 8.0% of control, $p < 0.01$) and amplitude (39.0% ± 8.5% of control, $p < 0.01$) of the electrical activity of MGC waves (Figures S4A, S4C, and S4D). However, considering the comparable suppression effects of CNQX on BC waves (Figures S4B–S4D; frequency: 51.0% ± 6.8% of control, $p < 0.01$; amplitude: 56.0% ± 9.2% of control, $p < 0.05$), the CNQX effects on the electrical activity of MGC waves may be largely due to its action on BCs. CNQX application had a larger suppressive effect on the amplitude of MGC waves than BC waves (MGC: 39.0% ± 8.5% of control; BC: 56.0% ± 9.2% of control; $p = 0.23$), suggesting that AMPA receptors of MGCs may also make a minor contribution to the electrical activities of MGC waves.

MGC Glutamate Transporters Play a Modulatory Role in Retinal Waves

To examine the role of the glutamate transporters of MGCs in retinal waves, we bath applied TFB-TBOA (1 μM) and found that blockade of glial glutamate transporters induced a long-lasting depolarization in MGCs within approximately 10 min (filled arrows, Figures 6A and 6B). This effect is possibly due to the accumulated glutamate in the extracellular space and then subsequent activation of AMPA receptors expressed on MGCs. Notably, there were no more MGC waves observed in all five cases examined later, after TFB-TBOA treatment (Figures 6A and 6C), suggesting that the glutamatergic signaling required for retinal waves is impaired by glutamate transporter blockade. Similarly, TFB-TBOA treatment also induced a large long-lasting activity in RGCs within 10 min (filled arrow, Figures 6D and 6E), and completely abolished RGC waves afterward in all five cases examined (Figures 6D and 6F). In addition, RGCs displayed a sustained inward current after the drug-induced long-lasting activity (open arrow, Figure 6D). Similarly, application of TFB-TBOA

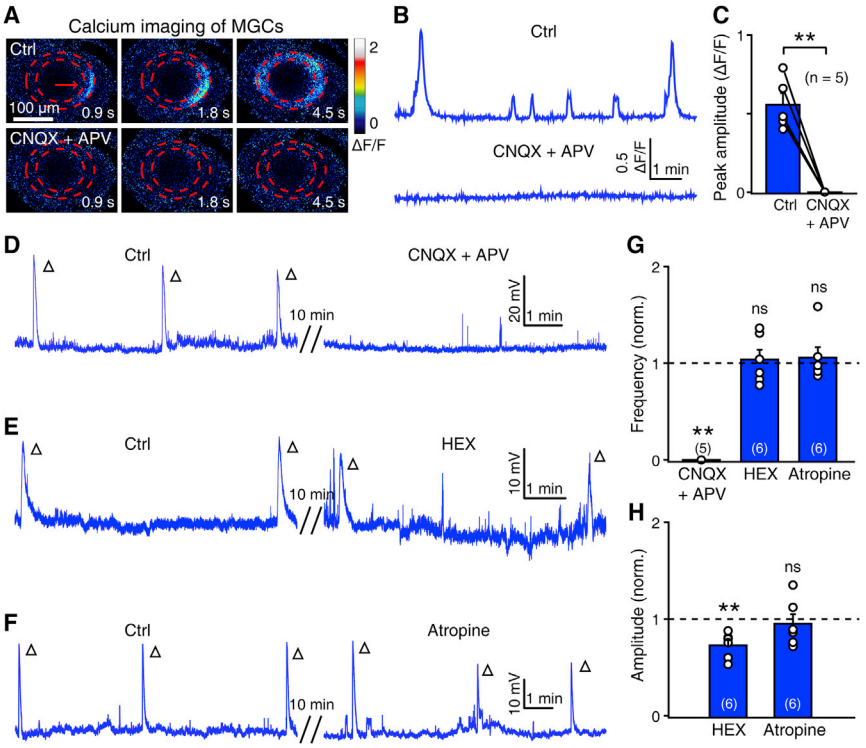

Figure 3. Calcium Waves of Müller Glial Cells Are Mainly Dependent on Glutamatergic Signaling

(A and B) Pseudocolor images (A) and calcium activities (B) showing the effect of CNQX (50 μM) + APV (50 μM) application on MGC calcium waves.

(C) Summary of data. The data obtained from the same larva are connected by a line.

(D–F) Example traces showing the effect of APV (50 μM) + CNQX (50 μM, D), HEX (100 μM, E), and atropine (2 μM, F) on the wave-like electrical activities of MGCs. Each open arrowhead represents an MGC wave.

(G and H) Summary of pharmacological effects on the frequency (G) and amplitude (H) of MGC waves.

The numbers in the brackets and on the bars indicate the numbers of larvae examined. The two-tailed paired Student's t test was performed for statistical analysis. ns, not significant; **p < 0.01. Data are represented as means ± SEMs.

at 0.1 or 0.2 μM significantly reduced the glutamate-induced responses of MGCs (Figures S5A and S5B; 50.7% ± 8.3% of control, $p < 0.05$) and induced a large inward current and abolished the waves in RGCs (Figures S5C–S5F). These results indicate that substantial blockade of MGC glutamate transporters may occlude retinal waves, possibly through elevating extracellular glutamate concentration.

We used a low dose of TFB-TBOA, 0.01 μM, which decreased the glutamate-induced responses of MGCs to a lesser degree in comparison with 0.1 μM (Figures S5A and S5B; 76.8% ± 4.5% of control, $p < 0.05$). We found that 0.01 μM TFB-TBOA significantly increased the amplitude of RGC waves (Figures 6G and 6H; 149.9% ± 15.2% of control, $p < 0.01$), but it did not change the wave frequency (Figures 6G and 6I; 108.4% ± 14.2% of control, $p = 0.4$). Moreover, application of TFB-TBOA at a range of 0.02–0.05 μM could induce spontaneous wave-like electrical activities in RGCs with no native wave (Figures S5G and S5H). These results suggest that partial blockade of MGC glutamate transporters may facilitate the occurrence of retinal waves.

This impairment of RGC waves by TFB-TBOA is not due to its effects on possible glutamate transporters expressed on RGCs themselves, because we found that the glutamate-induced responses of RGCs were not affected by TFB-TBOA (98.5% ± 5.2% of control, $p = 0.7$), but were largely suppressed by CNQX (37.0% ± 4.6% of control, $p < 0.01$) or APV (50.9% ± 9.0% of control, $p < 0.05$) (Figure S6). This is consistent with previous findings that there is no expression of EAAT1 and EAAT2 in the RGCs of larval zebrafish (Gesemann et al., 2010; Niklaus et al., 2017).

To examine whether functional enhancement of MGC glutamate transporters can downregulate retinal waves, we used GT949, which is a selective positive allosteric modulator of EAAT2 and can enhance glutamate uptake (Kortagere et al., 2018). Under blockade of synaptic transmission by adding Co^{2+} in the external solution, bath application of GT949 (0.1 μM) largely increased the glutamate-induced electrical responses of MGCs (Figures S7A and S7B, 148.1% ± 8.9% of control, $p < 0.05$), but did not significantly affect the responses of RGCs (Figures S7C and S7D, 98.4% ± 3.2% of control, $p = 0.5$), indicating the specific pharmacological action of GT949 on MGC glutamate transporters. Furthermore, application of GT949 largely reduced the amplitude of RGC waves (Figures 6J and 6K, 38.0% ± 8.5% of control, $p < 0.01$), although the frequency was not changed significantly (Figures 6J and 6L, 78.5% ± 17.1% of control, $p = 0.14$). These results suggest that glutamate transporters of MGCs play a modulatory role in the generation of retinal waves, possibly by controlling the level of extracellular glutamate.

DISCUSSION

In this study, by taking advantage of the optical transparency and small size of larval zebrafish retinae, we performed *in vivo* calcium imaging and whole-cell recording of MGCs and revealed that MGCs take part in retinal waves via glutamate transporters and AMPA receptors. Specifically, AMPA receptors mediate MGC calcium activities during retinal waves, whereas glutamate transporters play a modulatory role in retinal waves (Figure 7).

Two previous studies reported that MGCs exhibited spontaneous correlated activities with RGC waves during early developmental stages (Akrouh and Kerschensteiner, 2013; Rosa et al., 2015). Akrouh and Kerschensteiner (2013) showed that MGCs depolarize during each glutamatergic RGC wave by using dual whole-cell recordings from MGCs and RGCs. Rosa et al. (2015) showed that correlated calcium transients were observed at the stalk and lateral processes of MGCs and that these

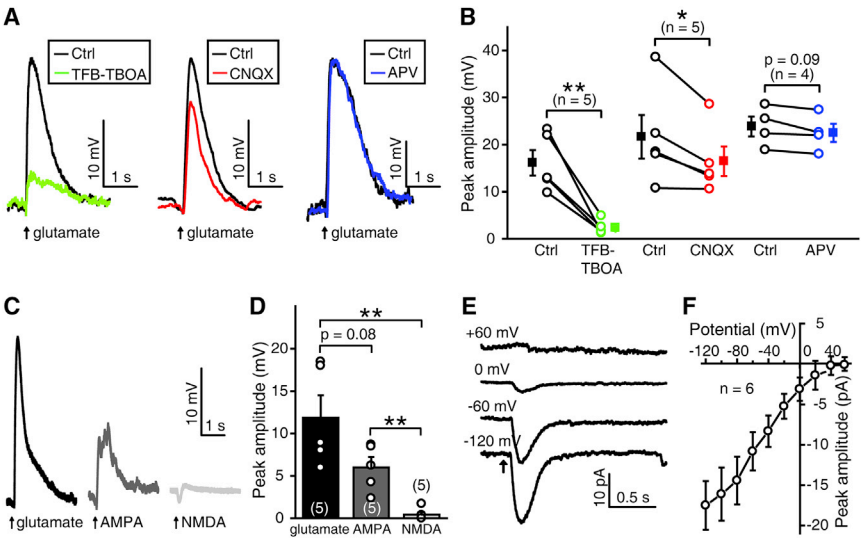

Figure 4. Glutamate-Induced Responses of Müller Glial Cells Are Mediated by Glial Glutamate Transporters and AMPA Receptors

(A) MGC responses evoked by local puffing of glutamate to MGC processes in the IPL under control (black), bath application of TFB-TBOA (1 μM) (green), bath application of CNQX (50 μM) (red), or bath application of APV (50 μM) (blue). MGCs were recorded under current-clamp mode, and synaptic transmission was blocked by adding Co^{2+} in the external solution.

(B) Summary of data. The data obtained from the same MGC are connected by a line.

(C) Electrical responses of an MGC under current-clamp mode when puffing of glutamate, AMPA, or NMDA at the processes of the MGC in the IPL.

(D) Summary of data.

(E) Glutamate-evoked MGC responses when the cell was held at the potential of −120, −60, 0, or +60 mV.

(F) Current-voltage plot showing MGC responses to glutamate at different holding potentials ranged from −120 to +60 mV with a step of 20 mV.

The numbers in the brackets and on the bars indicate the numbers of MGCs examined. The two-tailed paired Student's t test was used for data in (B) and the two-tailed unpaired Student's t test was used for data in (D). *p < 0.05, **p < 0.01. Data are represented as means ± SEMs.

activities are mediated by cholinergic or glutamatergic signals when retinal waves are cholinergic or glutamatergic, respectively, indicating that the responsiveness of MGCs matches the neurotransmitter used to generate RGC waves. In our previous study, retinal waves observed in zebrafish RGCs were found to be largely dependent on glutamatergic signaling and only slightly regulated by cholinergic signaling (Zhang et al., 2016). Here, we revealed that MGC waves consistently display properties that

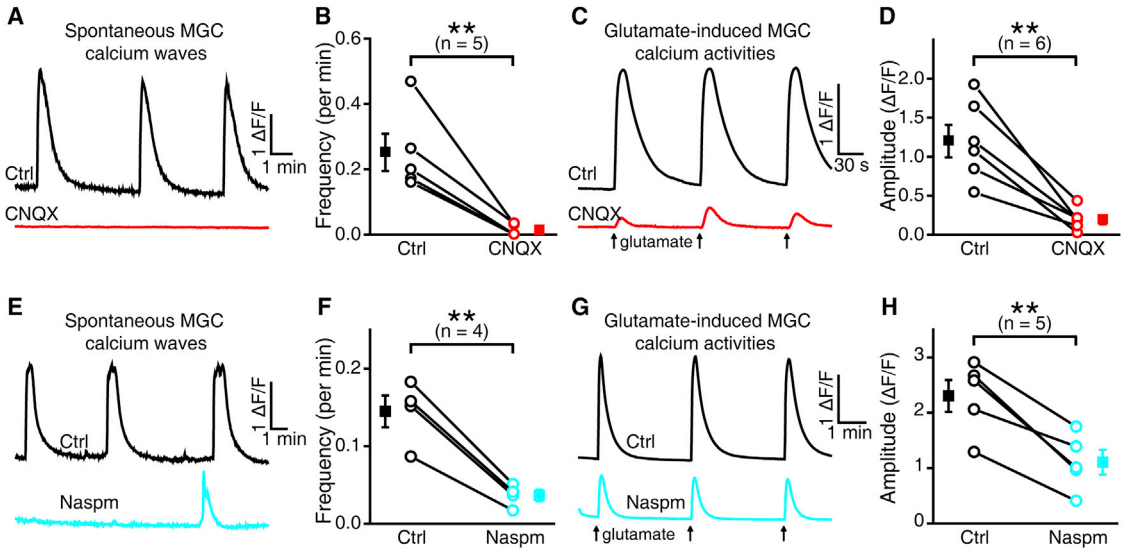

Figure 5. Calcium Waves of MGCs Are Mainly Mediated by Calcium-Permeable AMPA Receptors

(A) Spontaneous calcium activities of MGCs before (top) and after (bottom) bath application of CNQX (50 μM).

(B) Summary of data showing the CNQX effect on calcium waves of MGCs.

(C) Glutamate-induced calcium activities of MGCs before (top) and after (bottom) bath application of CNQX (50 μM).

(D) Summary of data showing the CNQX effect on glutamate-evoked calcium activities of MGCs.

(E) Spontaneous calcium activities of MGCs before (top) and after (bottom) bath application of Naspm (100 μM).

(F) Summary of data showing the effect of Naspm on calcium waves of MGCs.

(G) Glutamate-induced calcium activities of MGCs before (top) and after (bottom) bath application of Naspm (100 μM).

(H) Summary of data showing the effect of Naspm on glutamate-evoked calcium activities of MGCs.

The data obtained from the same larva are connected by a line, and the numbers in the brackets indicate the numbers of larvae examined. The Mann-Whitney test was used in (B), and the two-tailed paired Student's t test was used for data in (D), (F), and (H). **p < 0.01. Data are represented as means ± SEMs.

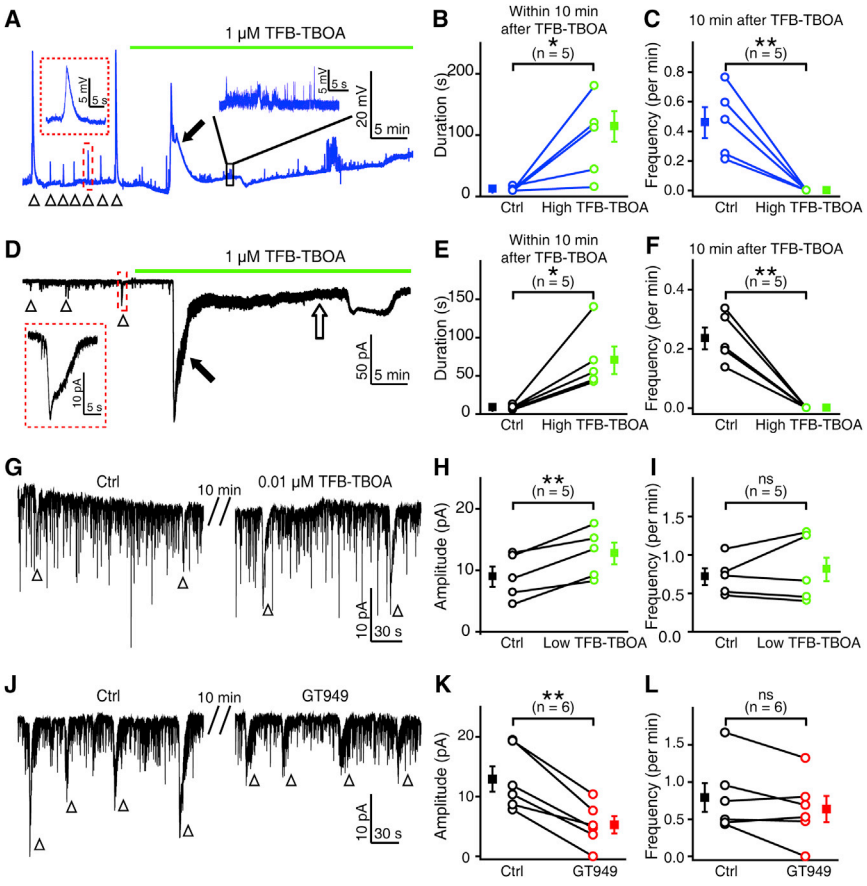

Figure 6. Modulation of Glial Glutamate Transporters Affects Retinal Waves

(A) Effects of high-dose TFB-TBOA application (1 μM) on spontaneous wave activities of MGCs. Inset, an enlarged wave activity in the red-boxed region. Arrowhead, wave-like activity; filled arrow, drug-induced long-lasting depolarization event. The trace in the black box was enlarged to show the small voltage fluctuations.

(B and C) Summary of data showing the change of MGC wave duration within 10 min after TFB-TBOA treatment (B), and the abolishment of MGC waves 10 min after TFB-TBOA application (C).

(D) Effects of high-dose TFB-TBOA application (1 μM) on spontaneous wave activities of RGCs. Inset, an enlarged wave activity in the red-boxed region. Arrowhead, wave-like activity; filled arrow, drug-induced long-lasting event; open arrow, drug-induced sustained inward current.

(E and F) Summary of data showing the change of RGC wave duration within 10 min after TFB-TBOA treatment (E), and the abolishment of RGC waves 10 min after TFB-TBOA application (F).

(G) Example traces showing the effect of low-dose TFB-TBOA (0.01 μM) on the spontaneous wave-like electrical activities of RGCs.

(H and I) Summary of data showing the effects of low-dose TFB-TBOA on the amplitude (H) and frequency (I) of RGC waves.

(J) Example traces showing the effect of GT949 (0.1 μM) on spontaneous wave-like electrical activities of RGCs.

(K and L) Summary of data showing the effect of GT949 on the amplitude (K) and frequency (L) of RGC waves.

The data obtained from the same cell are connected by a line, and the numbers in the brackets indicate the numbers of cells examined. The two-tailed paired Student's t test was used for statistical analysis. ns, not significant; *$p < 0.05$, **$p < 0.01$. Data are represented as means ± SEMs.

are similar to those of RGC waves in terms of neurotransmitter dependency.

What mediates the participation of MGCs in glutamatergic retinal waves? Rosa et al. (2015) found that glutamate-induced calcium activities at MGC processes in mice were largely reduced by blockade of AMPA but not NMDA receptors. We found that AMPA receptors but not NMDA receptors contribute to the electrical responses of MGCs evoked by glutamate (see Figures 4A–4C), and blockade of calcium-permeable AMPA receptors suppressed glutamate-induced calcium activities and abolished spontaneous calcium waves of MGCs (see Figure 5). It is reasonable that calcium-permeable AMPA receptors on MGCs can be activated by glutamate accumulated in the extracellular space during retinal waves, leading to an increase in the intracellular calcium ($[Ca^{2+}]_i$) of MGCs. Many lines of evidence showed that the $[Ca^{2+}]_i$ increase in glial cells may activate multiple intracellular signal pathways, trigger the release of gliotransmitters (e.g., glutamate, ATP, adenosine, D-serine), and modulate the activities of neighboring neurons or even vascular cells (Agulhon et al., 2008; Filosa et al., 2006; Khakh and McCarthy, 2015; Newman, 2015). At early developmental stages, MGC processes exhibit dynamic motility and almost occupy the exclusive spaces out of synaptic clefts in the retina (MacDonald et al., 2015; Williams et al., 2010). Therefore, it is of interest to investigate whether the $[Ca^{2+}]_i$ elevation of MGCs during retinal waves contributes to the release of gliotransmitters or vasoactive factors and regulates synaptic activities within the IPL or the constriction of blood vessels wrapped by MGC endfeet.

The EAAT1 and EAAT2 are two primary glia-specific glutamate transporters that have high affinity to glutamate and mediate >80% glutamate reuptake in the CNS (Bergles et al., 1997; Tzingounis and Wadiche, 2007). These two types of glutamate transporters can carry one molecule of glutamate in along with three Na^+ and one H^+ and can export one K^+, causing an inward current when translocating glutamate (Anderson and Swanson, 2000). Zebrafish glutamate transporters have multiple subtypes ranging from EAAT1 to EAAT7, of which EAAT1–5 show sequence and glutamate uptake function that are highly similar to those of humans and mice (Gesemann et al., 2010; Rico et al., 2010). Through *in situ* hybridization and immunostaining, a series of studies identified that EAAT2a and EAAT2b but not EAAT1 are expressed in the retina of larval zebrafish (Gesemann et al., 2010; Niklaus et al., 2017). Moreover, both EAAT2a and 2b subtypes are expressed in MGCs, but not in RGCs (Niklaus et al., 2017). TFB-TBOA, as a specific blocker of EAAT1 and EAAT2, consistently suppressed the

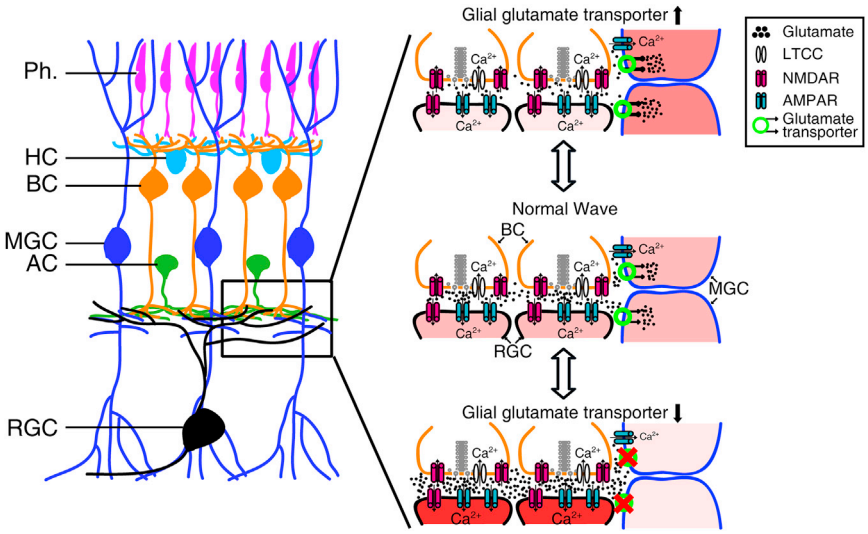

Figure 7. Schematic Model Showing the Participation and Function of MGCs in Retinal Waves

The glutamate released from BC axon terminals diffuses in the IPL with a wave-like manner and activates BCs and RGCs via ionotropic glutamate receptors and MGCs via glial glutamate transporters and AMPA receptors. AMPA receptors of MGCs mediate the calcium influx into MGCs. Facilitation of glial glutamate transporters on MGCs leads to re-uptake of more extracellular glutamate, restricting glutamate spillover and weakening retinal waves. Substantial blockade of glial glutamate transporters causes a large accumulation of extracellular glutamate, leading to the overactivation of RGCs and the occlusion of retinal waves.

glutamate-induced responses of MGCs, but it had no effect on RGCs (see Figures 4A–4C and S6). Glia-specific EAAT2 is believed to contribute to the majority of total glutamate uptake (Tanaka et al., 1997). Facilitation of EAAT2 function by GT949 can enhance glutamate uptake (Kortagere et al., 2018) and increase glutamate-induced responses of MGCs but not RGCs (see Figure S7). We found that GT949 application consistently decreased the amplitude of RGC waves (see Figures 6J and 6K), while partial blockade of EAAT2 by low doses of TFB-TBOA increased the wave amplitude or even induced spontaneous wave-like activities in RGCs with no native wave (see Figures 6G, 6H, S5G, and S5H). However, substantial blockade of MGC glutamate transporters by high doses of TFB-TBOA induced a large and sustained depolarization in both MGCs and RGCs (see Figures 6A, 6D, and S5C–S5F), indicating a large elevation in extracellular glutamate. Notably, following the sustained depolarization, there was no more wave in both RGCs and MGCs (see Figures 6A and 6D), suggesting that normal glutamatergic transmission may be impaired by substantial blockade of MGC glutamate transporters (Anderson and Swanson, 2000). Similar phenomena were observed when DL-threo-β-benzyloxyaspartate (DL-TBOA), a non-specific blocker of glutamate transporters, was applied (Zhang et al., 2016). A similar dose of DL-TBOA treatment increased the wave frequency but did not change the wave amplitude in the mouse retina (Blankenship et al., 2009). These different effects of glutamate transporter blockade on the waves in mice and zebrafish may be due to different expression patterns of glutamate transporter subtypes in retinal cells or to different sensitivities of glutamate transporters to TBOA in different species (Harada et al., 1998; Niklaus et al., 2017).

Glutamate transporters maintain extracellular glutamate at low concentrations, which are essential for protecting brain cells from excitotoxic injury and ensuring normal glutamatergic transmission (Huang and Bergles, 2004; Tzingounis and Wadiche, 2007). Glutamate transporter dysfunction and glutamate-mediated excitotoxicity have been found in many acute and chronic neural pathologies, including stroke, epilepsy, autism, traumatic brain injury, Huntington disease, and Alzheimer disease (Fontana, 2015). A series of compounds to enhance the expression or function of glutamate transporters has been developed for these pathological diseases (Kortagere et al., 2018; Rothstein et al., 2005). During retinal waves, a large amount of glutamate is released into the synaptic cleft and the extrasynaptic space from the axon terminals of BCs (Blankenship et al., 2009; Firl et al., 2013) and may reach several millimoles, which is harmful for cells in the inner retina (Zhou and Danbolt, 2014). There is a coincidence of increased expression of glutamate transporters and decreased propagation of retinal waves in developing retinae (Pannicke et al., 2002; Syed et al., 2004). The enhancement or impairment of the function of glutamate transporters consistently reduces or increases the wave amplitude (see Figures 6H and 6K). Therefore, through glutamate transporters and intimate enwrapping of synapses by their processes, MGCs can dynamically modulate retinal waves by controlling extracellular glutamate concentration (Miyazaki et al., 2017).

STAR★METHODS

Detailed methods are provided in the online version of this paper and include the following:

- KEY RESOURCES TABLE
- CONTACT FOR REAGENT AND RESOURCE SHARING
- EXPERIMENTAL MODEL AND SUBJECT DETAILS
  - Zebrafish
- METHOD DETAILS
  - *In Vivo* Calcium Imaging
  - *In Vivo* Whole-Cell Patch-Clamp Recording
  - Local Puffing of Drugs
- QUANTIFICATION AND STATISTICAL ANALYSIS
  - Statistical Analysis

SUPPLEMENTAL INFORMATION

Supplemental Information can be found online at https://doi.org/10.1016/j.celrep.2019.05.011.

ACKNOWLEDGMENTS

We are grateful to Dr. Pamela A. Raymond for providing the Tg(GFAP:eGFP) line and to Dr. Xiaoquan Li for making the Tg(GFAP:GCaMP2) line. This work was supported by the National Natural Science Foundation of China (31771144), the Key Research Program of Frontier Sciences (QYZDY-SSW-SMC028), the Strategic Priority Research Program (XDB32010200), the Youth Innovation Promotion Association of Chinese Academy of Sciences, Shanghai Municipal Science and Technology Major Project (18JC1410100 and 2018SHZDZX05), the China Wan-Ren Program, and the Shanghai Leading Scientist Program. The ORCID for R.-W.Z. is 0000-0003-1145-8589.

AUTHOR CONTRIBUTIONS

R.-W.Z. and J.-L.D. conceived the project and designed the experiments. R.-W.Z. and W.-J.D. performed the research and analyzed the data. D.A.P. provided some experimental reagents. R.-W.Z. and J.-L.D. wrote the paper.

DECLARATION OF INTERESTS

The authors declare no competing interests.

Received: July 23, 2018
Revised: February 21, 2019
Accepted: April 30, 2019
Published: June 4, 2019

REFERENCES

Ackman, J.B., and Crair, M.C. (2014). Role of emergent neural activity in visual map development. Curr. Opin. Neurobiol. *24*, 166–175.

Ackman, J.B., Burbridge, T.J., and Crair, M.C. (2012). Retinal waves coordinate patterned activity throughout the developing visual system. Nature *490*, 219–225.

Agulhon, C., Petravicz, J., McMullen, A.B., Sweger, E.J., Minton, S.K., Taves, S.R., Casper, K.B., Fiacco, T.A., and McCarthy, K.D. (2008). What is the role of astrocyte calcium in neurophysiology? Neuron *59*, 932–946.

Akrouh, A., and Kerschensteiner, D. (2013). Intersecting circuits generate precisely patterned retinal waves. Neuron *79*, 322–334.

Anderson, C.M., and Swanson, R.A. (2000). Astrocyte glutamate transport: review of properties, regulation, and physiological functions. Glia *32*, 1–14.

Bergles, D.E., Dzubay, J.A., and Jahr, C.E. (1997). Glutamate transporter currents in bergmann glial cells follow the time course of extrasynaptic glutamate. Proc. Natl. Acad. Sci. USA *94*, 14821–14825.

Bernardos, R.L., Barthel, L.K., Meyers, J.R., and Raymond, P.A. (2007). Late-stage neuronal progenitors in the retina are radial Müller glia that function as retinal stem cells. J. Neurosci. *27*, 7028–7040.

Blankenship, A.G., and Feller, M.B. (2010). Mechanisms underlying spontaneous patterned activity in developing neural circuits. Nat. Rev. Neurosci. *11*, 18–29.

Blankenship, A.G., Ford, K.J., Johnson, J., Seal, R.P., Edwards, R.H., Copenhagen, D.R., and Feller, M.B. (2009). Synaptic and extrasynaptic factors governing glutamatergic retinal waves. Neuron *62*, 230–241.

Budisantoso, T., Matsui, K., Kamasawa, N., Fukazawa, Y., and Shigemoto, R. (2012). Mechanisms underlying signal filtering at a multisynapse contact. J. Neurosci. *32*, 2357–2376.

Butts, D.A., Kanold, P.O., and Shatz, C.J. (2007). A burst-based "Hebbian" learning rule at retinogeniculate synapses links retinal waves to activity-dependent refinement. PLoS Biol. *5*, e61.

Droste, D., Seifert, G., Seddar, L., Jädtke, O., Steinhäuser, C., and Lohr, C. (2017). Ca^{2+}-permeable AMPA receptors in mouse olfactory bulb astrocytes. Sci. Rep. *7*, 44817.

Euler, T., Haverkamp, S., Schubert, T., and Baden, T. (2014). Retinal bipolar cells: elementary building blocks of vision. Nat. Rev. Neurosci. *15*, 507–519.

Filosa, J.A., Bonev, A.D., Straub, S.V., Meredith, A.L., Wilkerson, M.K., Aldrich, R.W., and Nelson, M.T. (2006). Local potassium signaling couples neuronal activity to vasodilation in the brain. Nat. Neurosci. *9*, 1397–1403.

Firl, A., Sack, G.S., Newman, Z.L., Tani, H., and Feller, M.B. (2013). Extrasynaptic glutamate and inhibitory neurotransmission modulate ganglion cell participation during glutamatergic retinal waves. J. Neurophysiol. *109*, 1969–1978.

Fontana, A.C. (2015). Current approaches to enhance glutamate transporter function and expression. J. Neurochem. *134*, 982–1007.

Ford, K.J., Félix, A.L., and Feller, M.B. (2012). Cellular mechanisms underlying spatiotemporal features of cholinergic retinal waves. J. Neurosci. *32*, 850–863.

Franze, K., Grosche, J., Skatchkov, S.N., Schinkinger, S., Foja, C., Schild, D., Uckermann, O., Travis, K., Reichenbach, A., and Guck, J. (2007). Muller cells are living optical fibers in the vertebrate retina. Proc. Natl. Acad. Sci. USA *104*, 8287–8292.

Gesemann, M., Lesslauer, A., Maurer, C.M., Schönthaler, H.B., and Neuhauss, S.C. (2010). Phylogenetic analysis of the vertebrate excitatory/neutral amino acid transporter (SLC1/EAAT) family reveals lineage specific subfamilies. BMC Evol. Biol. *10*, 117.

Halassa, M.M., and Haydon, P.G. (2010). Integrated brain circuits: astrocytic networks modulate neuronal activity and behavior. Annu. Rev. Physiol. *72*, 335–355.

Harada, T., Harada, C., Watanabe, M., Inoue, Y., Sakagawa, T., Nakayama, N., Sasaki, S., Okuyama, S., Watase, K., Wada, K., and Tanaka, K. (1998). Functions of the two glutamate transporters GLAST and GLT-1 in the retina. Proc. Natl. Acad. Sci. USA *95*, 4663–4666.

Huang, Y.H., and Bergles, D.E. (2004). Glutamate transporters bring competition to the synapse. Curr. Opin. Neurobiol. *14*, 346–352.

Katz, L.C., and Shatz, C.J. (1996). Synaptic activity and the construction of cortical circuits. Science *274*, 1133–1138.

Khakh, B.S., and McCarthy, K.D. (2015). Astrocyte calcium signaling: from observations to functions and the challenges therein. Cold Spring Harb. Perspect. Biol. *7*, a020404.

Kirkby, L.A., Sack, G.S., Firl, A., and Feller, M.B. (2013). A role for correlated spontaneous activity in the assembly of neural circuits. Neuron *80*, 1129–1144.

Kortagere, S., Mortensen, O.V., Xia, J., Lester, W., Fang, Y., Srikanth, Y., Salvino, J.M., and Fontana, A.C.K. (2018). Identification of Novel Allosteric Modulators of Glutamate Transporter EAAT2. ACS Chem. Neurosci. *9*, 522–534.

MacDonald, R.B., Randlett, O., Oswald, J., Yoshimatsu, T., Franze, K., and Harris, W.A. (2015). Müller glia provide essential tensile strength to the developing retina. J. Cell Biol. *210*, 1075–1083.

Malinow, R., and Malenka, R.C. (2002). AMPA receptor trafficking and synaptic plasticity. Annu. Rev. Neurosci. *25*, 103–126.

Meister, M., Wong, R.O., Baylor, D.A., and Shatz, C.J. (1991). Synchronous bursts of action potentials in ganglion cells of the developing mammalian retina. Science *252*, 939–943.

Miyazaki, T., Yamasaki, M., Hashimoto, K., Kohda, K., Yuzaki, M., Shimamoto, K., Tanaka, K., Kano, M., and Watanabe, M. (2017). Glutamate transporter GLAST controls synaptic wrapping by Bergmann glia and ensures proper wiring of Purkinje cells. Proc. Natl. Acad. Sci. USA *114*, 7438–7443.

Newman, E.A. (2015). Glial cell regulation of neuronal activity and blood flow in the retina by release of gliotransmitters. Philos. Trans. R. Soc. Lond. B Biol. Sci. *370*, 20140195.

Newman, E., and Reichenbach, A. (1996). The Müller cell: a functional element of the retina. Trends Neurosci. *19*, 307–312.

Niklaus, S., Cadetti, L., Vom Berg-Maurer, C.M., Lehnherr, A., Hotz, A.L., Forster, I.C., Gesemann, M., and Neuhauss, S.C.F. (2017). Shaping of Signal Transmission at the Photoreceptor Synapse by EAAT2 Glutamate Transporters. eNeuro *4*, ENEURO.0339-16.2017.

Pannicke, T., Bringmann, A., and Reichenbach, A. (2002). Electrophysiological characterization of retinal Müller glial cells from mouse during postnatal development: comparison with rabbit cells. Glia *38*, 268–272.

Peng, Y.W., Blackstone, C.D., Huganir, R.L., and Yau, K.W. (1995). Distribution of glutamate receptor subtypes in the vertebrate retina. Neuroscience *66*, 483–497.

Ramón y Cajal, S. (1972). The Structure of the Retina (Charles C Thomas).

Reichenbach, A., and Bringmann, A. (2013). New functions of Müller cells. Glia *61*, 651–678.

Rico, E.P., de Oliveira, D.L., Rosemberg, D.B., Mussulini, B.H., Bonan, C.D., Dias, R.D., Wofchuk, S., Souza, D.O., and Bogo, M.R. (2010). Expression and functional analysis of Na(+)-dependent glutamate transporters from zebrafish brain. Brain Res. Bull. *81*, 517–523.

Rosa, J.M., Bos, R., Sack, G.S., Fortuny, C., Agarwal, A., Bergles, D.E., Flannery, J.G., and Feller, M.B. (2015). Neuron-glia signaling in developing retina mediated by neurotransmitter spillover. eLife *4*, e09590.

Rothstein, J.D., Patel, S., Regan, M.R., Haenggeli, C., Huang, Y.H., Bergles, D.E., Jin, L., Dykes Hoberg, M., Vidensky, S., Chung, D.S., et al. (2005). Beta-lactam antibiotics offer neuroprotection by increasing glutamate transporter expression. Nature *433*, 73–77.

Schwartz, E.A., and Tachibana, M. (1990). Electrophysiology of glutamate and sodium co-transport in a glial cell of the salamander retina. J. Physiol. *426*, 43–80.

Snellman, J., Kaur, T., Shen, Y., and Nawy, S. (2008). Regulation of ON bipolar cell activity. Prog. Retin. Eye Res. *27*, 450–463.

Syed, M.M., Lee, S., Zheng, J., and Zhou, Z.J. (2004). Stage-dependent dynamics and modulation of spontaneous waves in the developing rabbit retina. J. Physiol. *560*, 533–549.

Tanaka, K., Watase, K., Manabe, T., Yamada, K., Watanabe, M., Takahashi, K., Iwama, H., Nishikawa, T., Ichihara, N., Kikuchi, T., et al. (1997). Epilepsy and exacerbation of brain injury in mice lacking the glutamate transporter GLT-1. Science *276*, 1699–1702.

Tsukada, S., Iino, M., Takayasu, Y., Shimamoto, K., and Ozawa, S. (2005). Effects of a novel glutamate transporter blocker, (2S, 3S)-3-[3-[4-(trifluoromethyl)benzoylamino]benzyloxy]aspartate (TFB-TBOA), on activities of hippocampal neurons. Neuropharmacology *48*, 479–491.

Tzingounis, A.V., and Wadiche, J.I. (2007). Glutamate transporters: confining runaway excitation by shaping synaptic transmission. Nat. Rev. Neurosci. *8*, 935–947.

Wei, H.P., Yao, Y.Y., Zhang, R.W., Zhao, X.F., and Du, J.L. (2012). Activity-induced long-term potentiation of excitatory synapses in developing zebrafish retina in vivo. Neuron *75*, 479–489.

Williams, P.R., Suzuki, S.C., Yoshimatsu, T., Lawrence, O.T., Waldron, S.J., Parsons, M.J., Nonet, M.L., and Wong, R.O. (2010). In vivo development of outer retinal synapses in the absence of glial contact. J. Neurosci. *30*, 11951–11961.

Wong, R.O. (1999). Retinal waves and visual system development. Annu. Rev. Neurosci. *22*, 29–47.

Yazulla, S., and Studholme, K.M. (2001). Neurochemical anatomy of the zebrafish retina as determined by immunocytochemistry. J. Neurocytol. *30*, 551–592.

Zhang, R.W., and Du, J.L. (2016). In Vivo Whole-Cell Patch-Clamp Recording in the Zebrafish Brain. Methods Mol. Biol. *1451*, 281–291.

Zhang, R.W., Wei, H.P., Xia, Y.M., and Du, J.L. (2010). Development of light response and GABAergic excitation-to-inhibition switch in zebrafish retinal ganglion cells. J. Physiol. *588*, 2557–2569.

Zhang, R.W., Li, X.Q., Kawakami, K., and Du, J.L. (2016). Stereotyped initiation of retinal waves by bipolar cells via presynaptic NMDA autoreceptors. Nat. Commun. *7*, 12650.

Zhou, Y., and Danbolt, N.C. (2014). Glutamate as a neurotransmitter in the healthy brain. J. Neural Transm. (Vienna) *121*, 799–817.

STAR★METHODS

KEY RESOURCES TABLE

REAGENT or RESOURCE	SOURCE	IDENTIFIER
Chemicals, Peptides, and Recombinant Proteins		
Alpha-Bungarotoxin	Tocris	Cat# 2133; CAS 11032-79-4
GT949	Tocris	Cat# 6578; CAS 460330-27-2
Naspm trihydrochloride	Tocris	Cat# 2766; CAS 1049731-36-3
TFB-TBOA	Tocris	Cat# 2532; CAS 480439-73-4
AMPA	Sigma-Aldrich	Cat #A6816; CAS 74341-63-2
Atropine	Sigma-Aldrich	Cat# A0132; CAS 51-55-8
CNQX	Sigma-Aldrich	Cat# C127; CAS 115066-14-3
Cobalt(II) chloride	Sigma-Aldrich	Cat# 232696; CAS 7646-79-9
DL-2-Amino-5-phosphonopentanoic acid	Sigma-Aldrich	Cat# A5282; CAS 76326-31-3
Hexamethonium chloride	Sigma-Aldrich	Cat# H2138; CAS 60-25-3
L-glutamate	Sigma-Aldrich	Cat# 49621; CAS 6106-04-3
L-(+)-2-Amino-4-phosphonobutyric acid	Sigma-Aldrich	Cat# A7929; CAS 23052-81-5
NMDA	Sigma-Aldrich	Cat# M3263; CAS 6384-92-5
Sulforhodamine 101	ThermoFisher	Cat# S359; CAS 60311-02-6
Experimental Models: Organisms/Strains		
Zebrafish: Tg(GFAP:eGFP); Sex: N/A; Age: 3 to 5 dpf	Bernardos et al., 2007	RRID: ZFIN-FISH-150901-29307
Zebrafish: Tg(GFAP:GCaMP2); Sex: N/A; Age: 3 to 5 dpf	This paper	N/A
Zebrafish: Tg(Ath5:gal4;UAS:mCherry); Sex: N/A; Age: 3 to 5 dpf	Zhang et al., 2016	RRID: ZDB-FISH-160511-4
Software and Algorithms		
MATLAB (electrophysiological data analysis)	MathWorks	https://www.mathworks.com
ImageJ (image analysis)	NIH	http://fiji.sc
Origin 8 (figure plotting)	OriginLab	https://www.originlab.com

CONTACT FOR REAGENT AND RESOURCE SHARING

Further information and requests for resources and reagents should be directed to and will be fulfilled by the Lead Contact, Rong-wei Zhang (rongweizhang@gmail.com).

EXPERIMENTAL MODEL AND SUBJECT DETAILS

Zebrafish

Adult zebrafish (*Danio Rerio*) were maintained in the National Zebrafish Resources of China (Shanghai, China) with an automatic fish-housing system at 28°C. Embryos and larvae were raised on a 14-10 h light-dark cycle in 10% Hank's solution, which consists of (in mM) 140 NaCl, 5.4 KCl, 0.25 Na_2HPO_4, 0.44 KH_2PO_4, 1.3 $CaCl_2$, 1.0 $MgSO_4$, and 4.2 $NaHCO_3$ (pH 7.2) (Zhang et al., 2010). Transgenic zebrafish lines used in this study include Tg(GFAP:eGFP), Tg(GFAP:GCaMP2), and Tg(Ath5:gal4; UAS:mCherry). All *in vivo* time-lapse two-photon imaging and whole-cell recording were performed on 3- to 5-dpf larvae at room temperature (22 - 26°C). For imaging experiments, 0.003% phenylthiourea (PTU) was added to the rearing solution to prevent pigmentation. All the experimental protocols were approved by the Animal Use Committee of Institute of Neuroscience, Chinese Academy of Sciences.

METHOD DETAILS

In Vivo Calcium Imaging

Tg(GFAP:GCaMP2) larvae were used for calcium imaging under a 40X objective (numerical aperture, N.A., 0.80) with an Olympus FV1000 confocal microscope (Olympus, Japan) equipped with a titanium: sapphire two-photon laser (Chameleon Ultra II, Coherent).

The laser was tuned to 900 nm for exciting GCaMPs. Imaging was performed on non-anaesthetized larvae, which were paralyzed with α-bungarotoxin (100 μg/ml) to prevent muscle contraction. Time-lapse images with a spatial resolution of 512 × 512 pixels were acquired at ~2 Hz.

For the experiments in Figures 5C, 5G, and S3, calcium imaging was performed under a 40X objective (numerical aperture, N.A., 0.80) with an Olympus BX51WI upright microscope, which was equipped with a digital camera OCRA-ER-1394 (Hamamatsu, Japan) for image acquisition, and a cyan light (470 ± 24 nm) of SPECTRA X light engine (Lumencor, USA) for illumination. The images were acquired via Micromanager version 1.4.15 (ImageJ, NIH) at 1 Hz. $CoCl_2$ (5 mM) was added in the bath to abolish synaptic transmission. All calcium imaging data were analyzed using ImageJ (NIH).

In Vivo Whole-Cell Patch-Clamp Recording

The preparation of zebrafish larvae and *in vivo* whole-cell recordings were performed according to our previous experimental procedures (Zhang and Du, 2016). The larvae were first paralyzed by 0.1% α-bungarotoxin for ~10 min, and then embedded in 1.2% low-melting agarose (Sigma) with one eye upward in a glass-bottomed chamber. The skin, cornea, and lens of the eye were removed by using a glass micropipette with a tip opening of 1 μm. After the dissection, the preparation was transferred to a electrophysiological setup, and continuously perfused with an extracellular solution, which consists of (in mM) 134 NaCl, 2.9 KCl, 4 $CaCl_2$, 10 HEPES and 10 glucose (290 mOsmol/L, pH = 7.8). *In vivo* whole-cell recordings of MGCs were performed on GFP-positive cells of Tg(GFAP:eGFP) larvae under fluorescent guidance and the recordings of RGCs were performed on the cell at the ganglion cell layer under DIC illumination. Recording micropipettes with a resistance of 15 - 25 MΩ were pulled with borosilicate capillaries (BF 100-58-10, Sutter Instruments) by using a Flaming/Brown P97 micropipette puller (Sutter Instruments). The micropipette was loaded with a low-chloride internal solution, which consists of (in mM) 100 K-gluconate, 10 KCl, 2 $CaCl_2$, 4 Mg_2ATP, 0.3 Na_4GTP, 10 HEPES, and 10 EGTA (280 mOsmol/L, pH = 7.4). Whole-cell recordings were made by a rupture of sealed membrane, and the data were filtered at 2.9 kHz and sampled at 10 kHz with an EPC-10 triple amplifier (HEKA, German).

Local Puffing of Drugs

For local application of drugs, a micropipette with a tip opening of ~2 μm was placed near MGC processes or RGC dendrites within the IPL. Drug-containing solution (Glutamate, 10 mM; AMPA, 1 mM; NMDA, 1 mM) was ejected out through a brief air pressure (100 ms in duration, 10 psi in pressure), which was controlled by a Picospritzer III (Parker Instrumentation).

QUANTIFICATION AND STATISTICAL ANALYSIS

Statistical Analysis

Lillietest function was first used to examine the normality distribution of data. For normal data of two-group comparison, two-tailed paired or unpaired Student's t test was used for significance analysis. Otherwise, non-parametric Mann-Whitney test was used. The p value less than 0.05 was considered to be statistically significant. All results were represented as mean ± SEM.

Cell Reports, Volume *27*

Supplemental Information

Müller Glial Cells Participate in Retinal Waves via Glutamate Transporters and AMPA Receptors

Rong-wei Zhang, Wen-jie Du, David A. Prober, and Jiu-lin Du

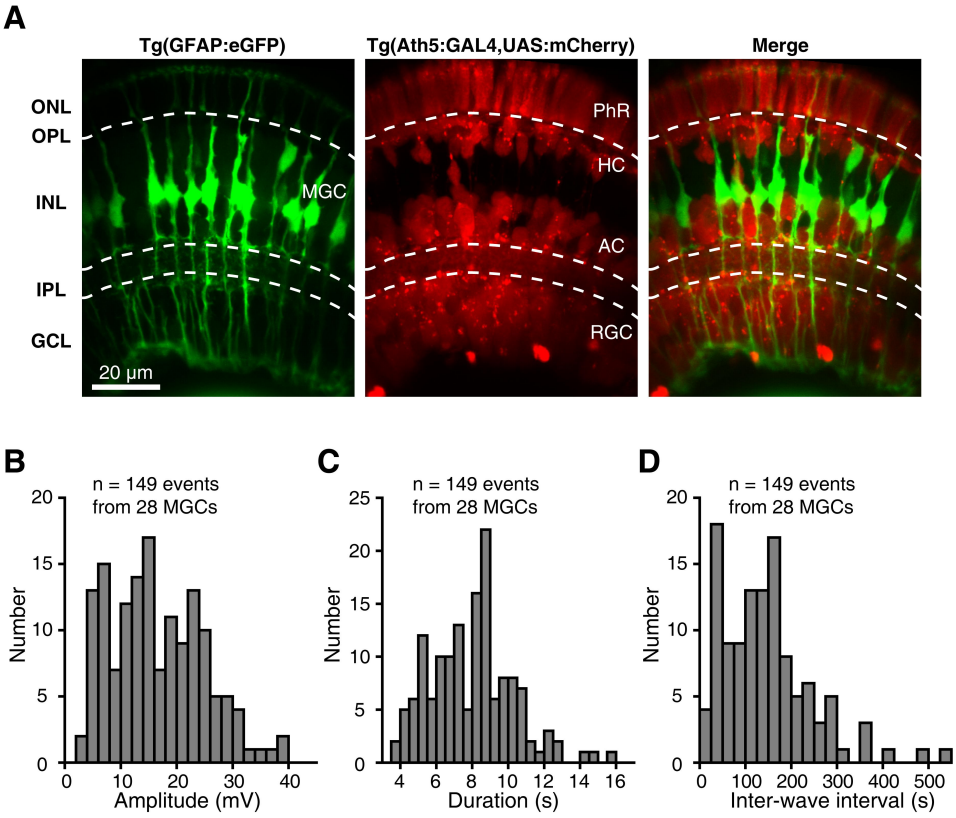

Figure S1. Morphology of MGCs and Characterization of MGCs' Wave-Like Spontaneous Electrical Activities in Zebrafish Larvae, Related to Figure 1.

(A) In vivo confocal images show MGCs and other retinal cells (including PhRs, HCs, ACs and RGCs) in a Tg(GFAP:eGFP,Ath5-gal4,UAS:mCherry) larva aged at 3 dpf. The top dash line indicates the location of the outer plexiform layer (OPL), and the bottom two lines indicates the boundaries of the inner plexiform layer (IPL). AC, amacrine cell; HC, horizontal cell; GCL, ganglion cell layer; INL, inner nuclear layer; MGC, Müller glial cell; ONL, outer nuclear layer; PhR, photoreceptor; RGC, retinal ganglion cell.

(B-D) Distribution of the amplitude (B), duration (C), and inter-wave interval (D) of spontaneous wave-like rhythmic electrical activities from 149 events in 28 MGCs at 3 dpf. Bin sizes: 2 mV (B), 0.5 s (C), 25 s (D).

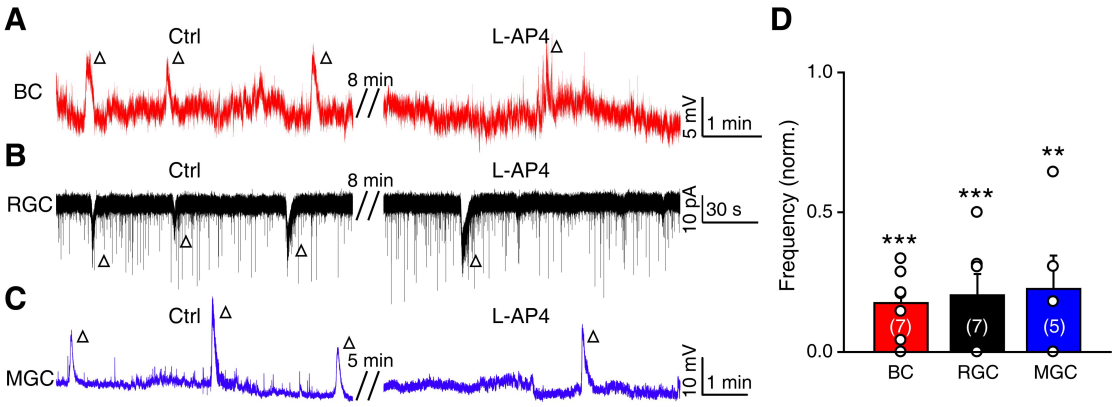

Figure S2. Activation of Type III Metabolic Glutamate Receptors Impairs Waves Activities in BCs, RGCs and MGCs, Related to Figure 3.

(A-C) Example traces showing spontaneous wave-like activities of a BC (A), a RGC (B), and a MGC (C) before (left) and after (right) bath application of L-AP4 (50 μM), an agonist of type III metabolic glutamate receptors. Each open arrowhead represents a wave-like event.

(D) Summary of data showing the effect of L-AP4 on the occurrence of waves in BCs, RGCs and MGCs. The wave frequency after L-AP4 application was divided by that before the drug application. Each dot indicates the data point from one cell.

The numbers on the bars indicate the numbers of cells examined. The two-tailed paired Student's *t*-test was used. **p < 0.01, ***p < 0.001. Data are represented as mean ± SEM.

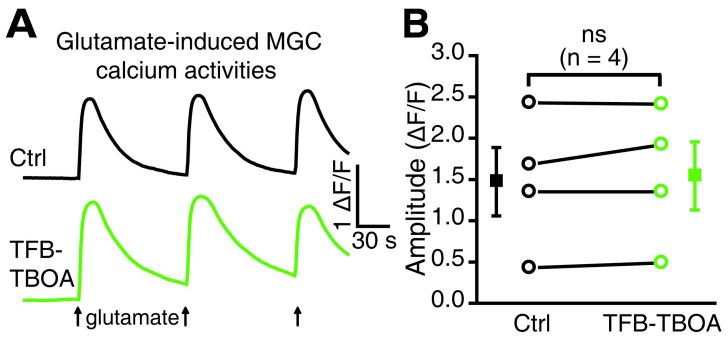

Figure S3. Calcium Waves of MGCs Are Not Dependent on Glial Glutamate Transporters, Related to Figure 5.

(A) Glutamate-induced calcium activities of MGCs before (top) and after (bottom) bath application of TFB-TBOA (1 μM).

(B) Summary of data showing the TFB-TBOA effect on glutamate-evoked calcium activities of MGCs.

The data obtained from the same larva are connected by a line, and the number in the brackets indicates the number of larvae examined. Two-tailed paired Student's *t*-test was used for data in (B). ns, not significant. Data are represented as mean ± SEM.

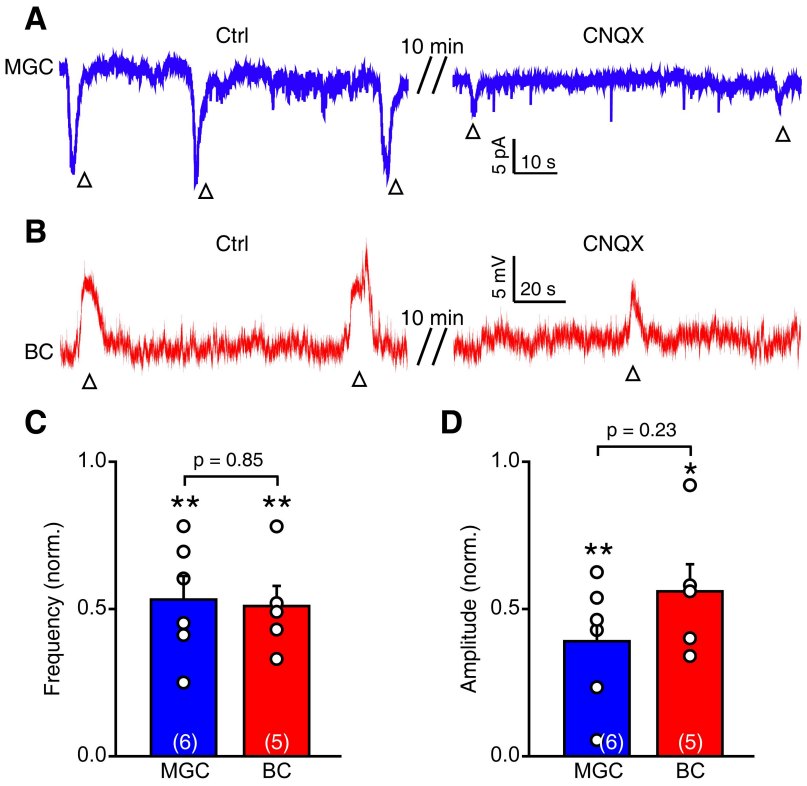

Figure S4. Blockade of AMPA Receptors Impairs the Electrical Activity of MGCs' and BCs' Waves, Related to Figure 4.

(A and B) Example traces showing spontaneous wave-like electrical activities of a MGC (A) and a BC (B) before (left) and after (right) bath application of CNQX (50 μM). Each open arrowhead represents a wave-like event.

(C and D) Summary of data showing the effects of CNQX on the frequency (C) and amplitude (D) of the electrical activities of MGCs' and BCs' waves.

The numbers on the bars indicate the numbers of cells examined. The two-tailed paired or unpaired Student's *t*-test was used for intra-group or inter-group comparison, respectively. *p< 0.05, **p< 0.01. Data are represented as mean ± SEM.

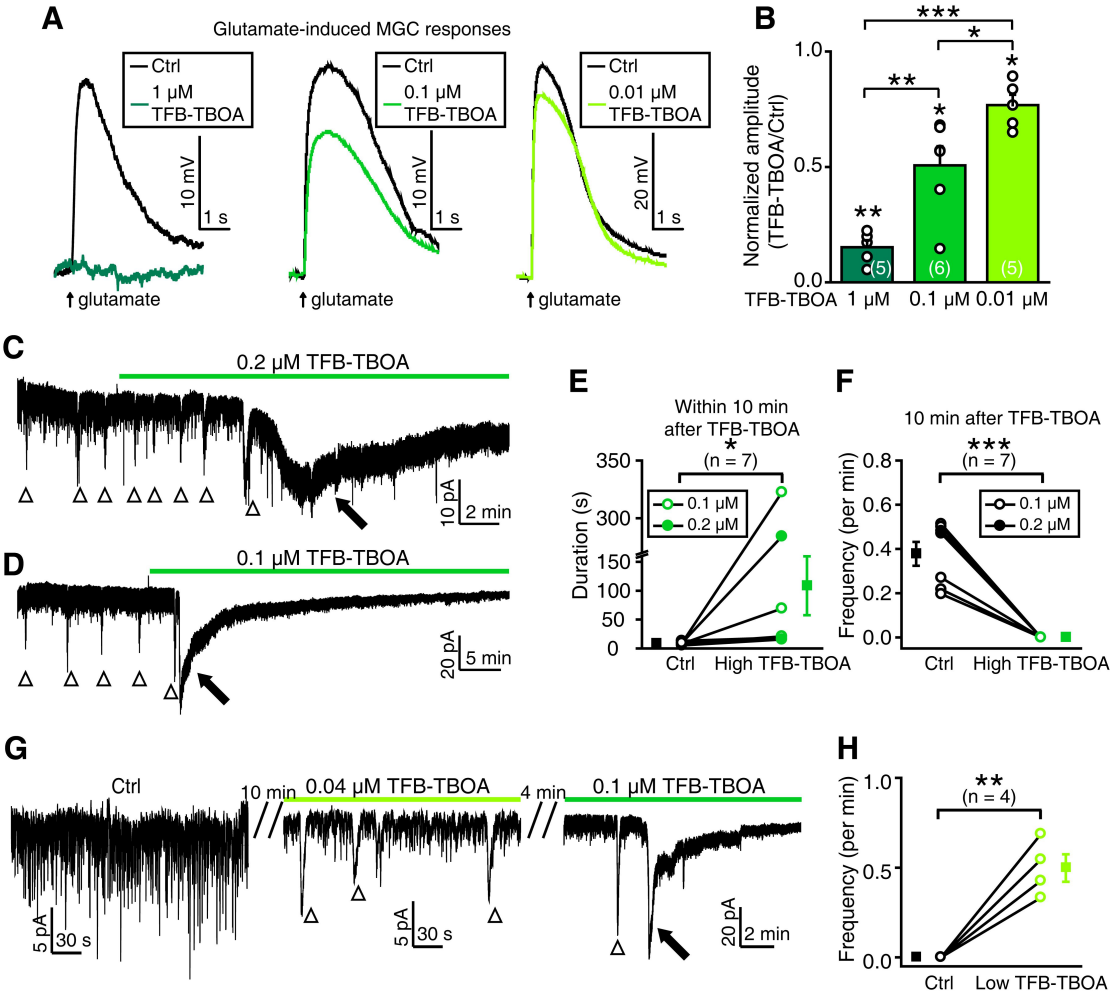

Figure S5. Different effects of High- and Low-Dose TFB-TBOA on Glutamate-Induced Responses of Müller Glial cells and Spontaneous Activities of RGCs, Related to Figure 6.

(A) MGC responses evoked by local puffing of glutamate to MGC processes in the IPL under different doses of TFB-TBOA (1 μM, 0.1 μM, and 0.01 μM). MGCs were recorded under current-clamp mode, and synaptic transmission was blocked by adding Co^{2+} in the external solution.

(B) Summary of data showing the effects of different doses of TFB-TBOA on glutamate-induced MGC responses. The data of 1-μM TFB-TBOA treatment was the same with those in Figure 4B.

(C and D) Effects of high-dose TFB-TBOA application (0.2 μM and 0.1 μM) on spontaneous wave activities of RGCs. Arrowhead, wave-like activity; filled arrow, drug-induced long-lasting inward current.

(E and F) Summary of data showing the change of RGC wave duration within 10 min after TFB-TBOA treatment (E), and the abolishment of RGC waves 10 min after TFB-TBOA application (F). The filled or open dots indicate 0.2- or 0.1-μM TFB-TBOA treatment, respectively.

(G) Example traces showing that low-dose TFB-TBOA (0.04 μM) induced wave-like electrical activities in the RGC with no native wave, while subsequent high-dose TFB-TBOA (0.1 μM) caused a long-lasting inward current (filled arrow). Notably, the scale bars are different among these traces.

(H) Summary of data showing that low-dose TFB-TBOA can facilitate the wave occurrence in RGCs with no native waves.

The numbers in the brackets and on the bars indicate the numbers of MGCs examined. The two-tailed paired or unpaired Student's *t*-test was used for intra-group or inter-group comparison in (B), respectively. The Mann-Whitney test was used for the data in (E), and the two-tailed paired Student's *t*-test was used for data in (F) and (H). *$p < 0.05$, **$p < 0.01$, ***$p < 0.001$. Data are represented as mean ± SEM.

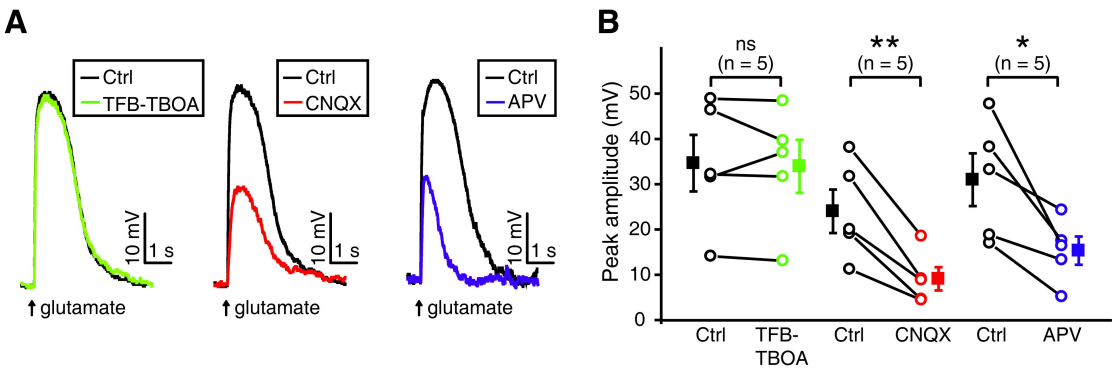

Figure S6. Glutamate-Induced Responses of RGCs Are Mediated by Ionotropic Glutamate Receptors But Not Glutamate Transporters, Related to Figure 6.

(A) RGC responses evoked by local puffing of glutamate to RGC dendrites in the IPL under control (black), bath application of TFB-TBOA (1 μM) (green), CNQX (50 μM) (red), or APV (50 μM) (blue). MGCs were recorded under current-clamp mode, and synaptic transmission was blocked by adding Co^{2+} in the external solution.

(B) Summary of data. The data obtained from the same RGC are connected by a line. The numbers in the brackets indicate the numbers of cells examined. The two-tailed paired Student's *t*-test was used for the data in (B). ns, not significant; *p< 0.05, **p< 0.01. Data are represented as mean ± SEM.

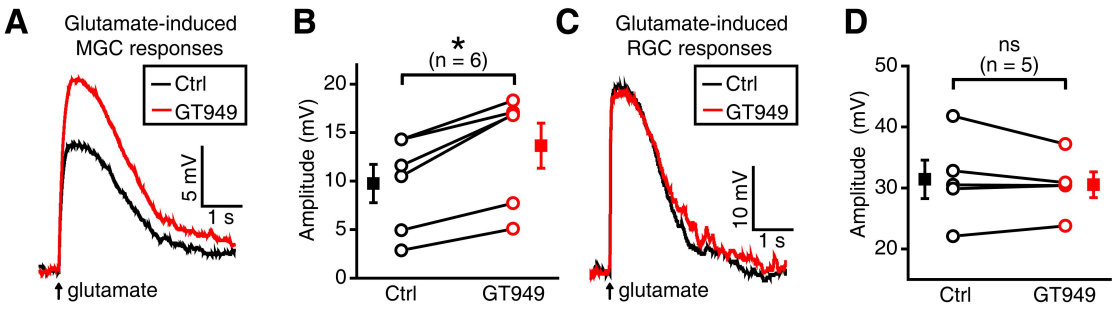

Figure S7. Effects of the Glial Glutamate Transporter Modulator GT949 on Glutamate-Induced Responses of MGCs and RGCs, Related to Figure 6.

(A) Effect of GT949 (0.1 μM) on glutamate-evoked electrical activities in MGCs. Here, CNQX was added in the bath to abolish the activation of AMPA receptors.

(B) Summary of data. The data obtained from the same MGC are connected by a line.

(C) Effect of GT949 (0.1 μM) on glutamate-evoked electrical activities in RGCs.

(D) Summary of data. The data obtained from the same RGC are connected by a line.

The numbers in the brackets indicate the numbers of cells examined. The Mann-Whitney test was used for the data in (B), and the two-tailed paired Student's *t*-test was used for data in (D). ns, not significant; *p< 0.05. Data are represented as mean ± SEM.